Acta Cryst. (1968). B**24**, 535

The Structure of Crystalline and Amorphous $CdGeP_2$

By R. Grigorovici and R. Mănăilă
Institute of Physics of the Academy, Bucharest, Romania

and A. A. Vaipolin
Institute of Technical Physics 'A.F.Ioffe', Leningrad, U.S.S.R.

(*Received* 24 *January* 1967 *and in revised form* 10 *April* 1967)

The structure of crystalline $CdGeP_2$ was refined by finding the phosphorus parameter $x=0{\cdot}283$. The radial distribution curve of amorphous $CdGeP_2$ was obtained by a diffractometric technique. From the shape of the first peak it could be inferred that the short-range order in the crystal is preserved in the amorphous and, presumably, in the molten phase.

Introduction

The ternary $A^{II}B^{IV}C_2^V$ compounds (where $A=Cd,Zn$; $B=Ge,Sn,Si$; $C=As,P$) are receiving more and more attention because of their interesting semiconducting properties. All these compounds belong to the space group $I\bar{4}2d$ (D_{2d}^{12}, chalcopyrite type). The arrangement that prevails in this structure is essentially a superlattice on that of zincblende. The structure is a tetrahedral one, every A or B atom being surrounded by four C atoms, while the C atoms have two A and two B atoms as nearest neighbours. The presence of two unequal shortest interatomic distances in the lattice (A–C and B–C) results in the distortion of the elemental tetrahedra, so that the c/a ratio is generally less than 2, the value which would be expected on the basis of atom ordering.

Recently Vaipolin, Goriunova, Osmanov & Rud (1965) obtained the vitreous (amorphous) form of $CdGeP_2$ and $CdGeAs_2$, a quite unusual form in compounds with strong covalent bonding. The glass was obtained by rapid quenching of the molten phase.

It seemed interesting to see to what extent the short-range order of the crystalline phase is preserved in the glassy phase. In particular we tried to find out whether the two distinct shortest interatomic distances in the crystal structure were maintained in the glass or if they were replaced by but one, because of some structural 'relaxation'. It is well known that the short-range order (number and distances of the nearest neighbours) controls the semiconducting properties of the material (Ioffe, 1947).

The structure of crystalline $CdGeP_2$

The structure of some $A^{II}B^{IV}C_2^V$ compounds was thoroughly studied by Pfister (1958, 1963), Folberth & Pfister (1957), Goodman (1957), Strauss & Rosenberg (1961), Gasson, Holmes, Jennings, Marathe & Parrott (1962), Leroux-Hugon (1963), Goriunova, Mamaev & Protchuchan (1962), Goriunova, Sokolova & Tsian Bin-Si (1963) and Tsian Bin-Si, Titchina, Osmanov & Goriunova (1963).

The crystalline $CdGeP_2$ has the lattice parameters $a=5{\cdot}740$, $c=10{\cdot}775$ Å (Vaipolin, Osmanov & Tretiakov, 1966). We undertook the refinement of this structure in order to be able to rely on it in our further consideration of the amorphous $CdGeP_2$.

The phosphorus parameter x was obtained from intensity measurements on powder samples.

In order to obtain a fine enough powder we employed fractional sedimentation in alcohol. The powder was then mounted on a glass substrate in a layer about 0·1 mm thick, the surface of which was smoothed out. In order to make the specimen coherent, the powder was mixed with a very dilute solution of celluloid in amyl acetate.

The diffraction pattern was obtained in a standard Debye–Scherrer camera ($\varphi=57{\cdot}3$ mm) with Cu $K\alpha$ radiation monochromatized by reflexion on a urea nitrate crystal. The primary beam met the specimen surface at a glancing angle of 80°.

In order to eliminate the L fluorescence radiation of Cd, the camera was loaded with two films superposed. The exposure time was selected so that the maximum density D should lie within the linear dependence region of D *versus* exposure.

The integrated intensities of the diffraction lines were measured by a photometric technique and corrected in the usual way for absorption, polarization and the Lorentz factor.

The use of a flat specimen allowed an exact knowledge of the absorption factor. The back-reflexion technique employed yielded sharp enough lines at all recorded diffraction angles.

The refinement of the structure required the intensity at high diffraction angles to be measured, as the higher h and k, the stronger the dependence of the intensity upon the phosphorus parameter x.

The method we used did not allow us to measure the weak diffraction lines. On the other hand, because of the rather poor resolving power, we could not measure separately the intensities of lines falling close to one another. Consequently, almost all the recorded lines are a superposition of several reflexions.

In order to find the phosphorus parameter x, we calculated the product of the structure and multiplicity factors pF^2 for the measured diffraction lines, by assuming in turn several x values.

The ratios of the calculated pF^2 were compared with the experimental ratios. For every x value the thermal Debye parameter B which enters the intensity factor $\exp[-2B(\sin\theta/\lambda)^2]$ was determined graphically. The experimental and calculated values pF^2 were scaled by using the equation $\Sigma\, pF^2_{\text{calc}} = \Sigma\, pF^2_{\text{exp}}$.

The usual R index cannot be employed here to characterize the accuracy of the determination. We resorted therefore to the factor

$$R' = \frac{\Sigma\,|pF^2_{\text{exp}} - pF^2_{\text{calc}}|}{\Sigma\, pF^2_{\text{exp}}}\,.$$

Table 1 displays the results of the calculation for four values given to x. On this basis we drew the $R'(x)$ dependence. The curve shows that the best agreement between the experimental and calculated values is obtained for $x=0{\cdot}283$.

The structure of amorphous $CdGeP_2$

Experimental procedure

In order to get some information about the short range order in amorphous $CdGeP_2$, we began by obtaining its electronic radial distribution curve by means of X-ray diffraction. We measured the X-ray intensity scattered at different angles by using a Siemens diffractometer, provided with a xenon-filled proportional counter.

The specimen consisted of finely ground $CdGeP_2$ powder (grain size less than 60 μm), pressed against a glass slide into a layer about 0·2 mm thick.

Table 1. *Observed and calculated pF^2 (per cent) versus phosphorus parameter x*

		$x=0{\cdot}270$		$x=0{\cdot}280$		$x=0{\cdot}290$		$x=0{\cdot}300$	
	hkl	pF_{calc}^2	pF_{exp}^2	pF_{calc}^2	pF_{exp}^2	pF_{calc}^2	pF_{exp}^2	pF_{calc}^2	pF_{exp}^2
(1)	408	56·4	48·0	48·3	45·8	43·3	45·1	42·4	45·1
(2)	532 1,0,11	66·9	54·8	58·7	52·3	54·5	51·5	55·4	51·5
(3)	329 600 525 516 444 611	86·6	91·5	81·4	87·4	81·2	86·0	87·8	86·0
(4)	428 3,1,10 437	81·3	82·5	79·0	78·8	79·9	77·5	85·7	77·5
(5)	2,1,11 613 419 620	42·7	40·7	38·0	38·9	33·8	38·3	30·5	38·3
(6)	604 0,0,12 541	40·1	39·7	35·9	37·9	32·3	37·3	29·8	37·3
(7)	615 536 624 2,0,12 631	100·0	100·8	100·0	96·3	100·0	94·8	100·0	94·7
(8)	3,3,10	17·0	17·2	17·7	16·4	17·7	17·1	17·1	16·1
(9)	448	21·6	23·0	21·7	21·9	20·3	21·6	17·2	21·6
(10)	617 552 712 4,1,11	41·5	44·9	45·1	42·9	46·9	42·2	45·3	42·2
(11)	529 640 635	7·9	18·9	11·0	18·1	14·5	17·8	16·7	17·8
	B	2·62		1·80		1·52		1·66	
	$R'(\%)$	8·1		6·1		6·9		8·9	

Two incident radiations were used: Cu *Kα* and Mo *Kα*. The former allowed us to record the intensities up to $s_m = 8{\cdot}1$, where $s_m = 4\pi \sin \theta_m/\lambda$. The Mo *Kα* radiation allowed an s_m as high as 17·3 to be attained and thus could be expected to offer a better resolution in the radial distribution curve.

The radiation was monochromatized by placing a β filter before the counter slit, but also, and primarily, by a suitable choice of the impulse height analyser channel. In order to find out the best position and width of this channel, we recorded the spectral distribution of the diffracted radiation by means of the same analyser, with the channel narrowed to 1 V. With both Cu *Kα* and Mo *Kα* radiations, the spectrograms showed a good deal of soft fluorescent radiation, which is to be assigned to Ge *Kα*, brought about by the incident short wavelength continuum.

Fig. 1 gives the spectral distribution of the Mo *Kα* radiation diffracted at $s = 3{\cdot}39$ by amorphous $CdGeP_2$ and by an amorphous quartz specimen. This value of s corresponds to the second diffraction maximum of $CdGeP_2$, but falls between the maxima of quartz. Although the characteristic radiation is preferentially diffracted into the maxima, the $CdGeP_2$ curve shows a much greater amount of soft radiation than the quartz one.

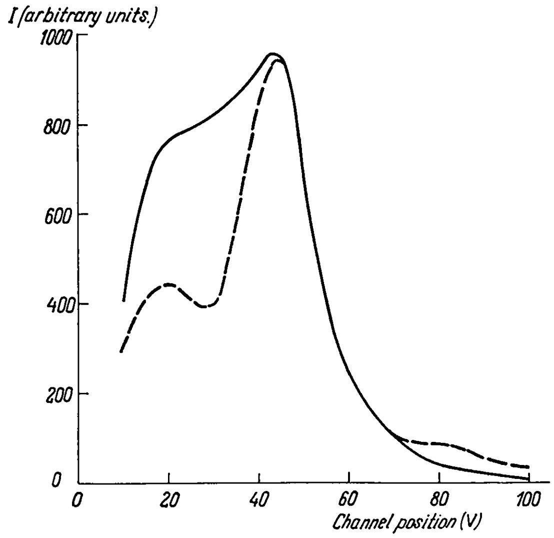

Fig. 1. Spectrograms of the diffracted Mo *Kα* radiation at $s = 3{\cdot}39$: (attenuator 100×). ——— from $CdGeP_2$. ------ from quartz.

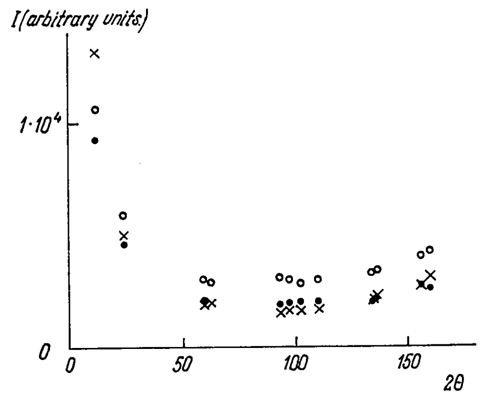

Fig. 2. Background intensity scattered by: ● Pd; × Al; ○ $CdGeP_2$.

Some spectrograms taken from $CdGeP_2$ at several diffraction angles showed this soft radiation to form a background rather irrespective of angle, as might be expected if fluorescence is involved.

According to these spectrograms, the channel position and width were chosen in every case so as to avoid as much as possible the recording of the soft radiation, even at high scattering angles.

The scattered intensity curve was taken point by point at equal intervals $\Delta s = 0{\cdot}1256$. The number of quanta recorded at each angle was never less than 1.10^3, corresponding to a probable relative error less than 2%.

The intensity data were firstly corrected for the fluorescence background. For the Cu *Kα* curve the following correction method was devised:

We recorded the intensity scattered by crystalline $CdGeP_2$, by Al and by Pd at several angles chosen so as to fall between the diffraction lines for all of these substances. The incident radiation was β-filtered and the 6V-wide analyser channel was centred upon 46V (attenuator 40×) which corresponds to the maximum of the Cu *Kα* radiation peak.

Fig. 2 displays the measured intensities *versus* 2θ. Excepting the first region, where the air and continuum effects may play an important role, it can be noticed that the points for Al and Pd fall close together, despite their very different atomic numbers. On the other hand the intensity scattered by crystalline $CdGeP_2$ is much higher, revealing a roughly angle-independent fluorescence background. Its value was subtracted from the intensity curve of amorphous $CdGeP_2$.

In the case of Mo *Kα* we estimated the background to be subtracted by taking into account the relative areas of the fluorescence and characteristic radiations on a high-angle spectrogram, for a given position and width of the analyser channel.

The second correction brought in allowed for the scattering by air. In order to carry out this correction we obtained the scattering curve of the air by merely taking aside the specimen holder, all the other recording conditions being kept the same. The air curve was then multiplied by a scaling factor of about 0·6 and subtracted from the $CdGeP_2$ scattering curve. The scaling factor was chosen so that the corrected scattering curve tended to zero when the scattering angle decreased to zero, as the maximum of order zero is not detectable at the lowest diffraction angle used in our measurements.

The intensity curve was then corrected for polarization. An essential advantage of the diffractometric method is that the absorption correction is independent of the scattering angle, so it could be left out.

Two such corrected intensity curves, obtained with Cu $K\alpha$ and Mo $K\alpha$ radiations are shown in Fig. 3.

The independent coherent scattering curve Σf^2 was calculated from the data of Cromer & Waber (1965), after applying to the f's the correction for anomalous dispersion (Cromer, 1965).

The experimental I_c curve was fitted at s about 16·3 to the theoretical one, composed of the independent coherent and the Compton scattering, so as to get the first part of the radial distribution curve ($r < 2{\cdot}5$ Å) as correct as possible.

The Fourier integration of the corrected intensity curve was performed by means of a Mader–Ott mechanical harmonic analyser.

Results and discussion

The electronic radial distribution curves of amorphous $CdGeP_2$ are displayed in Figs. 4 and 5. Both of them show a well enough resolved first peak at about 2·50 Å, corresponding to the Ge–P and Cd–P first coordinations.

Both these curves were constructed assuming the density of the amorphous phase to be equal to that of the crystalline one. A reduction in density of about 4·7% (by analogy with what happens in $CdGeAs_2$; Vaipolin *et al.*, 1965) would lead to a reduction of all ordinates and areas by a factor of 0·953.

The smallest interatomic distances in crystalline $CdGeP_2$ are the following:

Cd–P	2·55 Å
Ge–P	2·33
P–P	3·80
P–P	3·81
Cd–Cd = Ge–Ge = Cd–Ge	3·94
Cd–Ge	4·06
P–P	4·08
P–P	4·34 .

As can easily be seen, these distances fall into two main groups, which give rise to the first two peaks in the radial distribution curve of the amorphous material.

The interatomic distances in the crystal structure are represented in Fig. 4. The heights of the vertical lines indicate the relative weights of the interatomic distances.

The Mo $K\alpha$ intensity curve, integrated up to the same s_m as the Cu $K\alpha$ curve ($s_m = 8{\cdot}1$) yielded a radial distribution curve very similar to the Cu $K\alpha$ one (compare Fig. 6, chain-dotted curve, with Fig. 4). Moreover, when integrated up to $s_m = 14{\cdot}2$ (Fig. 5) it gives a radial distribution curve showing narrow, well resolved maxima. So we could abandon the Cu $K\alpha$ radial distribution curve, basing our further considerations only on that for Mo $K\alpha$.

However, care must be taken in analysing this curve, as the limited s_m introduces a number of secondary peaks, placed on each side of a real peak. As a matter of fact, by limiting the recorded intensity to a certain s_m, every well defined, δ-shaped coordination at a distance x_0 appears in the radial distribution curve as a

$$\frac{\sin [s_m(r-x_0)]}{s_m(r-x_0)} \tag{1}$$

function. The first secondary peak thus appears at $(5/4) \,.\, 2\pi/s_m$ on each side of a real one, followed by other peaks, spaced at $2\pi/s_m$. The height of the first secondary peak is about 13% of the real peak height.

These results are demonstrated in the first region of the radial distribution curve in Fig. 5, which reveals a

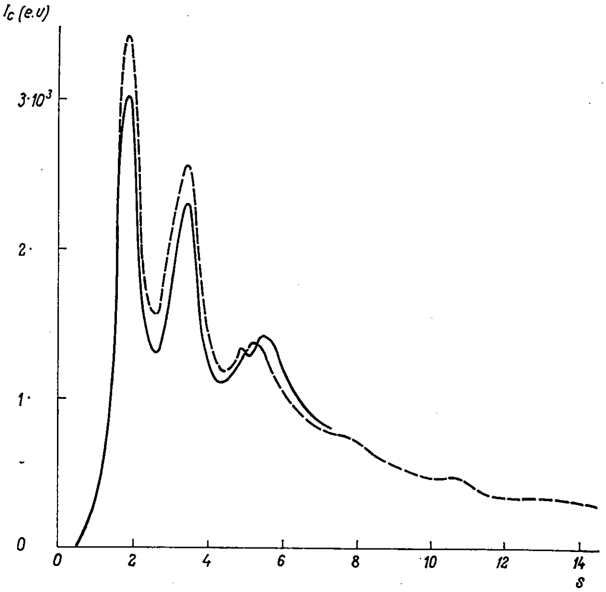

Fig. 3. Corrected scattered intensity curves from amorphous $CdGeP_2$, obtained with :——— Cu $K\alpha$; ------ Mo $K\alpha$.

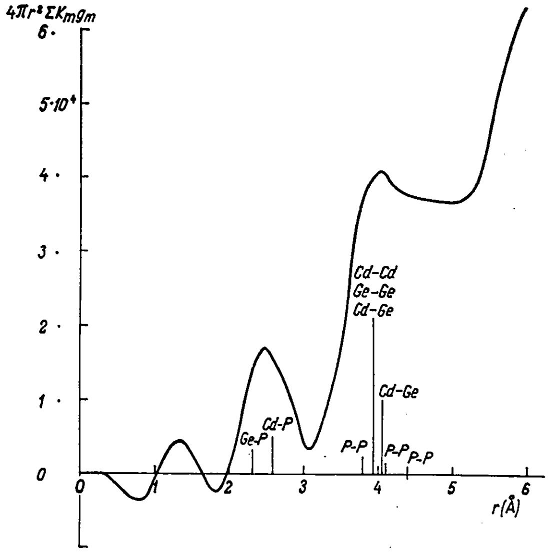

Fig. 4. Radial distribution curves of amorphous $CdGeP_2$ obtained with Cu $K\alpha$ radiation. The positions of the crystalline coordinations are also marked.

real peak placed at about 2·52 Å, surrounded by a series of secondary maxima. At $r > 3{\cdot}3$ Å the coordinations become very dense, so that different real and secondary maxima become superposed and cannot be resolved any more. Therefore we can get reliable information only concerning the first coordination sphere.

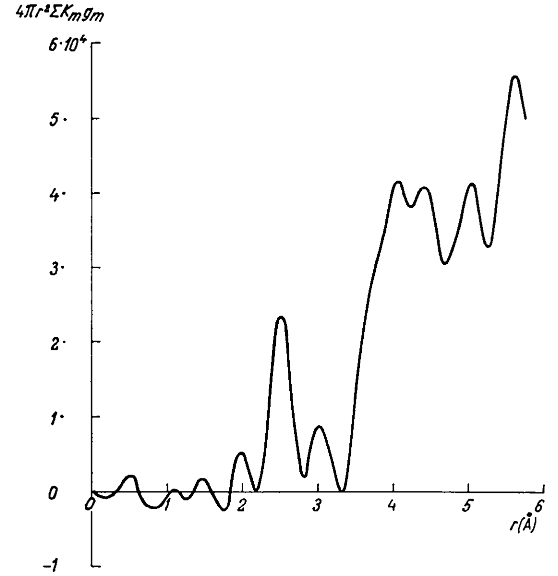

Fig. 5. Radial distribution curve of amorphous $CdGeP_2$ obtained with Mo $K\alpha$ radiation.

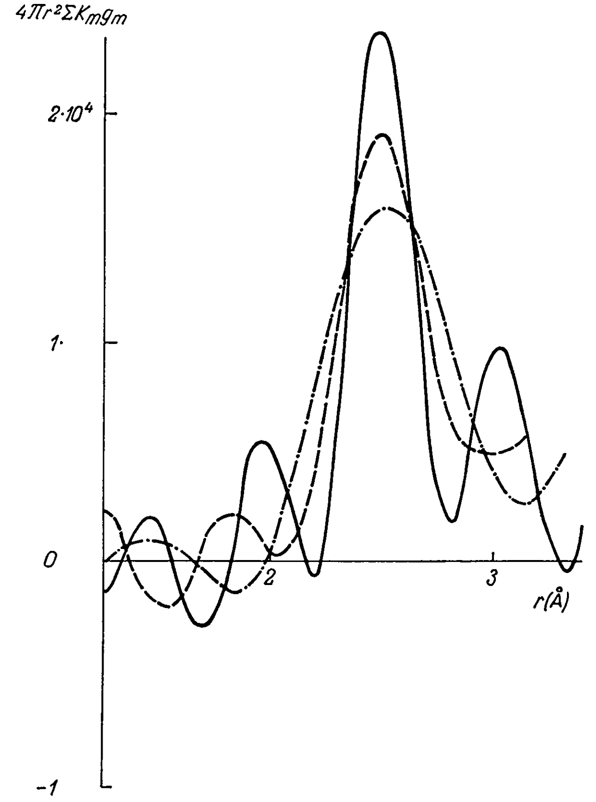

Fig. 6. The first region of the radial distribution curve obtained with Mo $K\alpha$. Length of the Fourier integration: -.-.-. $s_m = 8{\cdot}1$; ------ $s_m = 10{\cdot}9$; ——— $s_m = 14{\cdot}2$.

The correctness of the radial distribution curve may be checked by comparing the area of the first peak with the calculated one, on the assumption that the short-range order of the crystal is preserved. Theoretically:

$$A_T = 2 \times K_{\mathrm{Cd}} \times 4K_{\mathrm{P}} + 2 \times K_{\mathrm{Ge}} \times 4K_{\mathrm{P}} = 8K_{\mathrm{P}}(K_{\mathrm{Cd}} + K_{\mathrm{Ge}}) = 9060 \text{ e.u.},$$

where K_m is the effective number of electrons per atom of type m:

$$K_m = \frac{f_m}{f_e},$$

f_m and f_e being the scattering factors of the atom m and of a single electron respectively. We made use of the values:

$$K_{\mathrm{Cd}} = 50{\cdot}7$$
$$K_{\mathrm{Ge}} = 31{\cdot}9$$
$$K_{\mathrm{P}} = 13{\cdot}7\,.$$

The experimental area was taken as twice the area under the radial distribution curve from $r = 0$ to $r = 2{\cdot}52$ Å, so allowing for the secondary maxima, which reduce the area under the central peak. This procedure was required by the fact that the shape of the radial distribution curve is not rigorously a sin x/x one, since, as will be further shown, the first coordination is not strictly localized but rather enlarged. Consequently, the ratio 1·18 between the area of the central peak and the total area under the curve is no more preserved and we can rely only upon the total area, which is preserved. On the other hand, the region above 2·50 Å is affected by contributions from higher coordinations.

For three integration lengths: $s_m = 8{\cdot}1$, 10·9, 14·2 (Fig. 6), the total area was equal respectively to 9350, 9200, 8550 e.u. After allowing for the smaller density of the amorphous material, the areas became: 8910, 8770, 8150 e.u., somewhat smaller than the theoretically predicted one.

The shape of the first peak in the radial distribution curve may give very useful information about the nature of the short-range order. The question we are interested in is whether the two shortest interatomic distances in the lattice are preserved in the amorphous material, or whether they are blended together by some kind of structural 'relaxation'.

Fig. 6 displays the first part of the radial distribution curve for the three integration lengths. It is easy to show that the first peak is much too wide as compared with the theoretical function (1) for all three integration lengths. We tried to account for this fact by supposing that every coordination at $x = x_0$ in the lattice is broadened in the amorphous material into a Gaussian distribution:

$$\exp\left[-(x - x_0)^2/c^2\right].$$

This kind of broadened coordination was first suggested by Voigtlaender-Tetzner (1958).

The radial distribution function arising from such a coordination will be:

$$[4\pi r^2 \Sigma K_m g_m]_{x_0} = k\int_0^\infty \exp\left[-(x-x_0)^2/c^2\right] \frac{\sin[s_m(r-x)]}{s_m(r-x)}\,dx\,, \quad (2)$$

k being related to the total area of the peak. The curve may be thought of as composed of many such contributions superposed.

In order to check this method in the simpler case of an elementary amorphous substance, we tried to build up the first radial distribution peak of amorphous Ge relying on the coordination distances found in the crystal. Fig. 7 displays the result between 2 and 3 Å of superposing three Gaussian coordinations centred on 2·5, 4·2 and 4·6 Å, possessing c-parameter values of 0·27, 0·6 and 1·0 respectively. These coordinations were weighted by the number of neighbours to be found in each of them. These higher coordinations had to be taken into account because of their above-mentioned influence at smaller r. The experimental curve was obtained by us with Cu $K\alpha$ radiation ($s_m = 8$) on amorphous, vacuum-evaporated Ge layers. As can be seen, the agreement is satisfactory. This fact confirms the assumption about the Gaussian broadening of the coordinations in amorphous materials.

We computed the integral in (2) for several values of c lying between 0 and 1. The relative maximum intensity I_m/I_{m0} and half-height width Δ/Δ_0 of the first peak are plotted in Fig. 8, curves a, *versus* the parameter c, for $s_m = 8$. In order to use this dependence for other values of s_m we must pay attention to the relations

$$I_m \sim s_m\,, \quad \Delta \sim 1/s_m$$

by carrying out every time the reduction of the data to $s_m = 8$. The experimental results are summarized in Table 2 (first three columns), for the three curves of Fig. 6. c_I and c_Δ denote the broadening parameters resulting from the intensity and width data, according to the curves a of Fig. 8.

It can easily be seen that the c_Δ are much larger than the c_I, showing that our radial distribution peak is too wide to be accounted for by a single interatomic distance.

Consequently, we tried to fit our experimental data to a superposition of two coordinations, Δr apart. The heights of the two coordinations were weighted by K_{Cd} and K_{Ge} respectively.

The I_m/I_{m0} and Δ/Δ_0 curves were calculated for $\Delta r =$ 0·1, 0·2 and 0·3 Å. The results are plotted in Fig. 8 as curves b. The c values we got by fitting the experimental data to the three Δr are given in Table 2.

It is obvious that the experimental data fit much better with two interatomic distances than with but one. It is, however, impossible to decide which value of Δr offers the best agreement.

Table 3, which is based on Table 2, gives the relative differences between $\bar{c}_I$ and $\bar{c}_\Delta$, as well as the mean deviation $|\overline{\Delta c}|/\bar{c}$ of the c values, averaged over both $\bar{c}$'s. The $\bar{c}_I$ are averaged over the three s_m.

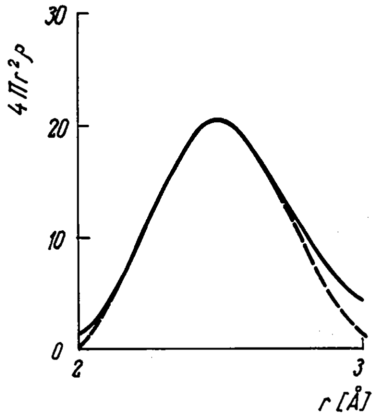

Fig. 7. Fitting of the first radial distribution curve peak of amorphous Ge to a superposition of Gaussian coordinations: ——— observed; ------ calculated.

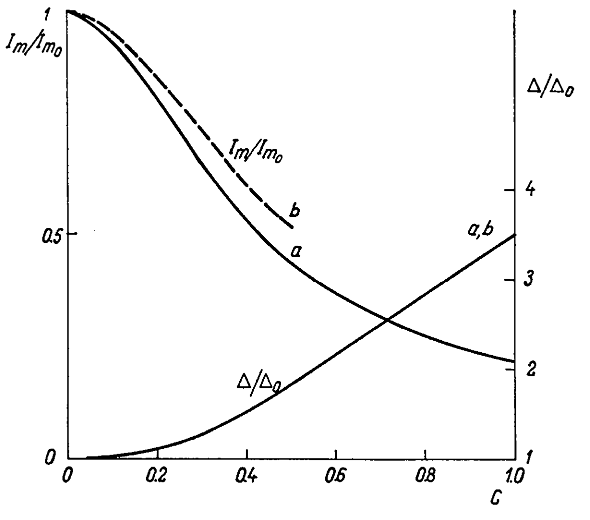

Fig. 8. Relative maximum intensity and relative width of the peak *versus* the broadening parameter c (calculated).

Table 2. *Values of c parameter in case of two broadened coordinations Δr apart*

s_m	$\Delta r = 0$ c_I	$\Delta r = 0$ c_Δ	$\Delta r = 0·1$ Å c_I	$\Delta r = 0·1$ Å c_Δ	$\Delta r = 0·2$ Å c_I	$\Delta r = 0·2$ Å c_Δ	$\Delta r = 0·3$ Å c_I	$\Delta r = 0·3$ Å c_Δ
8·1	0·309	0·791	0·259	0·360	0·220	0·330	0·144	0·275
10·9	0·366	0·730	0·319	0·317	0·292	0·275	0·230	0·220
14·2	0·381	0·665	0·336	0·272	0·315	0·205	0·262	0·230

It may be seen that $\Delta r \neq 0$ gives values of c_I and c_Δ close to each other, but, as the mean deviation of both of them exceeds the differences between $\bar{c}_I$ and $\bar{c}_\Delta$, it is impossible for us to decide upon the most probable Δr.

On the other hand, we noticed that the variation of c_I and c_Δ with s_m in Table 2 shows a certain trend, which agrees with the already mentioned trend in the first peak areas. It might be attributed to the inherent errors that the long integrations introduce into the r.d. curve.

Table 3. *Mean deviations of the c values for several Δr*

Δr (Å)	$\frac{\bar{c}\Delta - \bar{c}}{\bar{c}} I-$	$\frac{\lvert\overline{\Delta c}\rvert}{\bar{c}}$
0	0·676	0·093
0·1	0·036	0·132
0·2	0·022	0·201
0·3	0·019	0·314

Conclusions

The structure of crystalline $CdGeP_2$ was refined by a photographic technique. The phosphorus parameter x was found to be as high as 0·283.

The electronic radial distribution curve was obtained for amorphous $CdGeP_2$ by using a diffractometric technique and two different incident wavelengths. By considering the shape of the first peak in the radial distribution curve it could be inferred that the distances Cd–P and Ge–P differ, as is the case in the crystalline structure too.

Consequently, in the amorphous $CdGeP_2$ every phosphorus atom preserves its four nearest neighbours, two Cd and two Ge atoms, at slightly different distances. This shows that in this phase, and presumably also in the liquid phase, from which the amorphous phase proceeds, the character of the bonds is as covalent as in the crystalline structure (see also Nikol'skaia, Berger, Efimovski, Kagirova & Shukina, 1966). This enables us to think that the molten phase must possess semiconducting properties, as these have been shown to depend in the first instance on the short-range order.

It is a pleasure to thank Prof. N.A. Goriunova for continuous interest and helpful discussions and Dr I.I. Titchina for providing the material used in this study.

References

CROMER, D. T. (1965). *Acta Cryst.* **18**, 17.
CROMER, D. T. & WABER, J. T. (1965). *Acta Cryst.* **18**, 104.
FOLBERTH, O. G. & PFISTER, H. (1957). *Halbleiter und Phosphore*, p. 474. Braunschweig: Vieweg.
GASSON, D. B., HOLMES, P. J., JENNINGS, I. C., MARATHE, B. R. & PARROTT, J. E. (1962). *J. Phys. Chem. Solids*, **23**, 1291.
GOODMAN, C.H.L. (1957). *Nature, Lond.* **179**, 828.
GORIUNOVA, N. A., MAMAEV, S. M. & PROTCHUCHAN, V. D. (1962). *Dokl. Akad. Nauk SSSR*, **142**, 623.
GORIUNOVA, N. A., SOKOLOVA, V. I. & TSIAN BIN-SI (1963). *Dokl. Akad. Nauk SSSR*, **152**, 363.
IOFFE, A. F. (1947). *Iubilneii Sbornik Akad. Nauk SSSR*, p. 305.
LEROUX-HUGON, P. (1963). *C.r. Acad. Sci. Paris*, **256**, 118.
NIKOL'SKAIA, G. F., BERGER, L. I., EFIMOVSKI, I. V., KAGIROVA, G. N., SHUKINA, I. K. & KOVALEVA, I. S. (1966). *Neorganicheskie materialy*, **2**, 1876.
PFISTER, H. (1958). *Acta Cryst.* **11**, 221.
PFISTER, H. (1963). *Acta Cryst.* **16**, 153.
STRAUSS, A. J. & ROSENBERG, A. J. (1961). *J. Phys. Chem. Solids*, **17**, 278.
TSIAN BIN-SI, TITCHINA, I. I., OSMANOV, E. O. & GORIUNOVA, N. A. (1963). Reports of the 21st Scientific Conf. L.I.S.I.-Leningrad, Physics Sect., p. 8.
VAIPOLIN, A. A., GORIUNOVA, N. A., OSMANOV, E. O. & RUD, YU. V. (1965). *Dokl. Akad. Nauk SSSR*, **160**, 633.
VAIPOLIN, A. A., OSMANOV, E. O. & TRETIAKOV, P. N. (1967). *Neorganicheskie materialy*, **2**, 1876.
VOIGTLAENDER-TETZNER, G. (1958). *Z. Physik*, **150**, 215.